A decoupled strategy to solve reduced-order multimodel problems in the PGD and Arlequin frameworks

David Néron, Hachmi Ben Dhia, Régis Cottereau

A decoupled strategy to solve reduced-order multimodel problems in the PGD and Arlequin frameworks

David Néron[a,*], Hachmi Ben Dhia[b], Régis Cottereau[b]

[a] *LMT-Cachan (ENS Cachan/CNRS/Université Paris-Saclay)*
61 avenue du Président Wilson, 94235 Cachan Cedex, France

[b] *MSSMat (CentraleSupélec/CNRS/Université Paris-Saclay)*
Grande Voie des Vignes, 92295 Châtenay-Malabry Cedex, France

Abstract

In this paper, we investigate the coupling of reduced models for the simulation of structures involving localized geometrical details. Herein, we use the Arlequin method, originally designed to deal with multimodel and multiscale analyses of mechanical problems, to mix reduced models built using the Proper Generalized Decomposition. Instead of solving the global coupled problem in a monolithic way, the LATIN strategy is used to propose a decoupled algorithm. The numerical examples demonstrate the feasibility of the approach and in particular its potentiality in terms of flexibility.

Keywords: reduced-order modeling, PGD, multimodel, multiscale, Arlequin, LATIN

1. Introduction

In engineering design, the numerical simulation of very large multiscale models is becoming increasingly important because of the need to describe realistic scenarios and to derive tools to facilitate the virtual design of new structures. However, the incredible evolution of computing resources over the last decade is balanced by the increasing complexity of the models that engineers want to address in their efforts to design, control and optimize innovative products. Solving several problems with very large number of degrees of freedom, with the presence of multiscale and multiphysics aspects, or with the need to take

*Corresponding author
Email address: neron@elmt.ens-cachan.fr (David Néron)

into account uncertainties or parameter variations cannot be handled by standard solution techniques. In this context, model reduction methods have a huge potential to develop innovative tools for intensive computation and allow a "real time" interaction between the user and the simulations, which gives the opportunity to explore a large number of scenarios in the design office.

Several approaches of reduced-order modeling have been proposed, many of them relying on the assumption of a separated form of the unknowns. A first family of algorithms starts by a learning phase (performing some preliminary computations, called *snapshots*) to build a reduced-order basis that allows to capture the principal characteristics of the solution of the problem to be solved. It is the case of the methods based on the Proper Orthogonal Decomposition (see e.g. [1, 2, 3, 4]) or of the Reduced Basis method (see e.g. [5, 6]). The latter adds an automatic selection of the snapshots by a greedy algorithm based on some efficient error indicators. Another family follows a different path as it builds progressively an approximate separated representation of the solution, without assuming any basis or selecting any snapshots. It is the case of the Proper Generalized Decomposition (PGD, see e.g. [7, 8] or [9] for a review of the method) which was considered in our former works, in particular for the analysis of elastic-viscoplastic problems [10], multiscale problems [11] or parametrized studies [12]. This method has also been widely developed by Chinesta and coauthors who proposed very efficient implementations of the approach and a large variety of applications (see [13] for an overview). To focus only on some recent examples, one can cite real-time simulations in surgery [14, 15], real-time monitoring of thermal process [16] or the simulation of viscoelastic models [17].

However, to move a step forward, a major issue which is addressed herein is the coupling of reduced-order models to mix several models within the same simulation. This point is exemplified by Figure 1, which represents a holed square structure with different shapes. The brute force classical approach to evaluate the influence of the shape of the hole is to mesh the structure for each geometry and run the simulation, possibly using a reduced modeling strategy that generates modes specific to this particular geometry.

The approach which is explored in this paper is different. We propose to superpose two reduced models: one for the global structure and one for the local detail (see Figure 2). This would allow a considerable increase in the flexibility of the solution and provide new opportunities in terms of design, such as:

- the ability to consider a complete system as an assembly of components, each represented by its own model;
- the possibility of handling reduced models arising from several actors involved in the design of the same product;
- the ability to take into account the critical phenomena, which occur locally

in time and space, with a finer numerical model that could be adapted automatically during the simulation;

- the flexibility to change some local data (geometry, topology, material, architecture ...) in order to change the global structure.

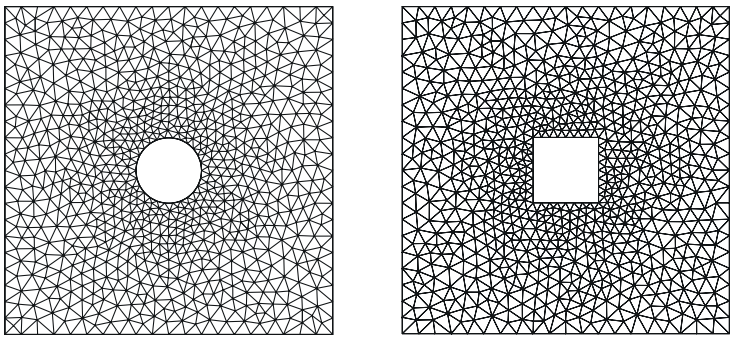

Figure 1: Remeshing global structure involving a local geometrical detail

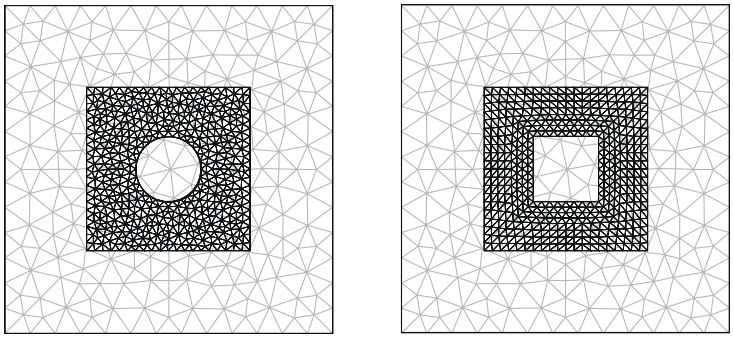

Figure 2: Superposition of local models in a single global model

The issue of coupling reduced models is essentially the possibly different natures of the mathematical models to "marry", that is the management of incompatibilities between the models. This question was addressed in [18, 19] for multiphysics problems such as thermo-poroelasticity. In these works, based on the concept of "interface between physics", the LATIN method was used to solve in a decoupled manner the problems corresponding to the different physics, and the PGD was applied to reduce the computational cost of the models.

In this paper, we propose to use the Arlequin technique [20]. This technique has been designed to deal with problems in which several "zones" of interest can be distinguished and require different levels of analysis. The term "zones" should be understood in the broad-sense, as it concerns different numerical models whose fields can be mixed and glued together. For that, a superposition technique based on a weak formulation, in which the energy is distributed

between the various models is used. This technique allows to deal with incompatible models, including the ones defined on different meshes. The Arlequin method has been the subject of many developments (see e.g. [21, 22, 23]) and showed its capabilities to locally refine models to introduce an essential local modification in models.

The Arlequin modeling framework has already been used in [24] in the context of the PGD. In this work, the technique was implemented to split a complex physical geometry in rather simple ones, in order to allow a separation of the geometrical coordinates. The different simple zones were then solved using the PGD approximation introduced in the global formulation, allowing a strong decrease of the computational cost.

Herein, the aim is different. It consists in transforming the classical weak-Arlequin volume coupling into a strong (pointwise) coupling. This local coupling between models allows for the use of the LATIN algorithm as a decoupled solver and the implementation of the PGD technique for each of the overlapping models. This approach leads to an interesting flexibility as it will permit at the end, to use different PGD solvers, dedicated to the specificities of the models that are considered (linear/nonlinear, deterministic/stochastic, atomistic/continuum ...) as well as, in the future, resorting to precomputed reduced-models stored in a library.

The present paper is organized as follows. In Section 2, the framework of the Arlequin strategy is recalled in the case of linear elasticity and reformulated to be solved by a decoupled algorithm. In Section 3, the LATIN algorithm is introduced to solve the problem in a decoupled manner. The PGD approach is then used to solve the problems corresponding to the different models. Finally, some numerical examples are proposed in Section 4 to illustrate the behavior of the strategy.

2. Arlequin formulation

Only the main features of the approach are recalled herein. For further details, especially on the theoretical aspects, the interested reader can refer to [22]. In order to recall the Arlequin formulation, we consider the following representative model.

2.1. Classical linearized elasticity problem

Let us consider the evolution over the time interval $I = (0, T)$ of an elastic body occupying the closure of a bounded regular domain Ω_1 included in $\mathbb{R}^d$,

with $d = 1, 2$ or 3 in practice. It is submitted to a field of volume density of forces $\boldsymbol{f}$, a field of surface density of forces $\boldsymbol{F}$ on Γ_F, a part of its boundary, and clamped on Γ_u, a non zero measured other part of the boundary (see Figure 3).

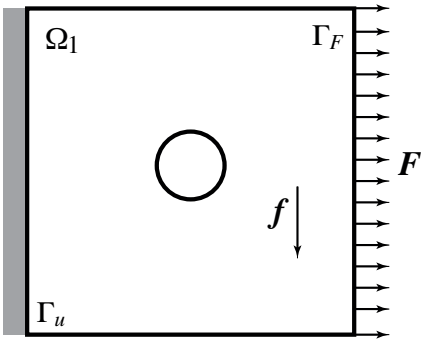

Figure 3: Reference problem

For a given space $\boldsymbol{V}$, we denote $L^2(I;\boldsymbol{V}) = \{\boldsymbol{v} : I \to \boldsymbol{V}\ ;\ \int_I ||\boldsymbol{v}||^2_{\boldsymbol{V}} dt < +\infty\}$ and $||\cdot||_{\boldsymbol{V}}$ a norm on $\boldsymbol{V}$. Then, we introduce $\boldsymbol{V}_0 = \{\boldsymbol{v} \in \boldsymbol{H}^1(\Omega_1)\ ;\ \boldsymbol{v} = \boldsymbol{0} \text{ on } \Gamma_u\}$ and we define $\boldsymbol{W}_0 = L^2(I;\boldsymbol{V}_0)$, $\boldsymbol{F}_0 = L^2(I;\boldsymbol{L}^2(\Omega_1))$ and $\boldsymbol{G}_0 = L^2(I;\boldsymbol{L}^2(\Gamma_F))$. If we assume that $\boldsymbol{f} \in \boldsymbol{F}_0$ and $\boldsymbol{F} \in \boldsymbol{G}_0$, the displacement field $\boldsymbol{u}_0$ is a function of $(\boldsymbol{x}, t) \in \Omega_1 \times I$ and the weak primal (*monomodel*) formulation of this problem reads as follows:

$$\begin{gathered}\text{Find } \boldsymbol{u}_0 \in \boldsymbol{W}_0\ ;\\ \forall\, \boldsymbol{v}_0 \in \boldsymbol{W}_0, \quad a_0(\boldsymbol{u}_0, \boldsymbol{v}_0) = \ell_0(\boldsymbol{v}_0)\end{gathered} \tag{1}$$

where the virtual works of the internal and external forces respectively read:

$$\forall\, (\boldsymbol{u}_0, \boldsymbol{v}_0) \in \boldsymbol{W}_0 \times \boldsymbol{W}_0, \quad a_0(\boldsymbol{u}_0, \boldsymbol{v}_0) = \int_{\Omega_1} \boldsymbol{\sigma}(\boldsymbol{u}_0) : \boldsymbol{\varepsilon}(\boldsymbol{v}_0)\, d\Omega \tag{2}$$

$$\forall\, \boldsymbol{v}_0 \in \boldsymbol{W}_0, \quad \ell_0(\boldsymbol{v}_0) = \int_{\Omega_1} \boldsymbol{f} \cdot \boldsymbol{v}_0\, d\Omega + \int_{\Gamma_F} \boldsymbol{F} \cdot \boldsymbol{v}_0\, dS \tag{3}$$

In these equations, $\boldsymbol{\varepsilon}(\boldsymbol{v}_0)$ and $\boldsymbol{\sigma}(\boldsymbol{v}_0)$ denote the linearized strain and stress tensors, associated to field $\boldsymbol{v}_0$, which are assumed to be connected through a Hooke's law.

2.2. Lagrange multiplier-based Arlequin formulations of the elasticity problem

Let Ω_2 be a non-zero measured given bounded regular domain overlapping Ω_1. Let Ω_{12} be the overlap. For clarity and with no major restrictions, it will be assumed that Ω_2 is strictly embedded in Ω_1, leading to $\Omega_{12} = \Omega_2$. The overlap

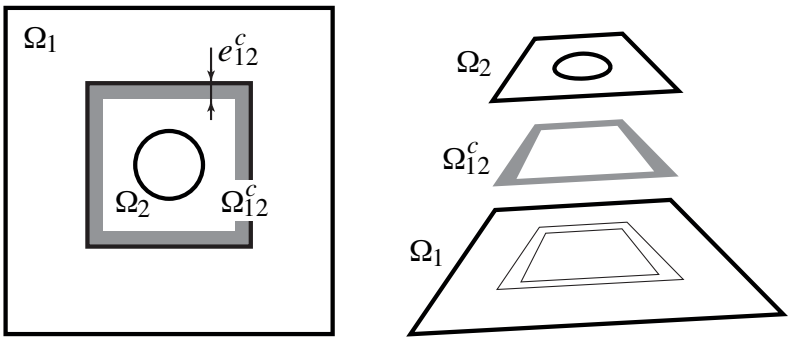

Figure 4: Arlequin models and the coupling zone (in grey)

is partitioned into two regular non overlapping domains, i.e. $\Omega_{12} = \Omega_{12}^c \cup \Omega_{12}^f$ where Ω_{12}^c is the models gluing zone (see the grey zone in Figure 4).

Now, to define Arlequin formulations of the elasticity problem, we denote by $\boldsymbol{W}_1 = L^2(I; \boldsymbol{V}_1)$ with $\boldsymbol{V}_1 = \{\boldsymbol{v} \in \boldsymbol{H}^1(\Omega_1)\ ;\ \boldsymbol{v} = \boldsymbol{0} \text{ on } \Gamma_u\}$ and $\boldsymbol{W}_2 = L^2(I; \boldsymbol{V}_2)$ with $\boldsymbol{V}_2 = \boldsymbol{H}^1(\Omega_2)$. Weighted internal and external virtual works are defined by:

$$\forall\, (\boldsymbol{u}_1,\, \boldsymbol{v}_1) \in \boldsymbol{W}_1, \quad a_1(\boldsymbol{u}_1, \boldsymbol{v}_1) = \int_{\Omega_1} \alpha_1\, \boldsymbol{\sigma}(\boldsymbol{u}_1) \boldsymbol{:} \boldsymbol{\varepsilon}(\boldsymbol{v}_1)\, d\Omega \tag{4}$$

$$\forall\, (\boldsymbol{u}_2,\, \boldsymbol{v}_2) \in \boldsymbol{W}_2, \quad a_2(\boldsymbol{u}_2, \boldsymbol{v}_2) = \int_{\Omega_2} \alpha_2\, \boldsymbol{\sigma}(\boldsymbol{u}_2) \boldsymbol{:} \boldsymbol{\varepsilon}(\boldsymbol{v}_2)\, d\Omega \tag{5}$$

$$\forall\, \boldsymbol{v}_1 \in \boldsymbol{W}_1, \quad \ell_1(\boldsymbol{v}_1) = \int_{\Omega_1} \alpha_1\, \boldsymbol{f} \cdot \boldsymbol{v}_1\, d\Omega + \int_{\Gamma_F} \alpha_1\, \boldsymbol{F} \cdot \boldsymbol{v}_1\, dS \tag{6}$$

$$\forall\, \boldsymbol{v}_2 \in \boldsymbol{W}_2, \quad \ell_2(\boldsymbol{v}_2) = \int_{\Omega_2} \alpha_2\, \boldsymbol{f} \cdot \boldsymbol{v}_2\, d\Omega \tag{7}$$

where weight parameter functions (α_1, α_2) are defined respectively in Ω_1 and Ω_2 and satisfy (see Figure 5) for $i = 1, 2$:

$$\alpha_i \geqslant 0 \quad \text{in} \quad \Omega_i, \quad \alpha_i = 1 \quad \text{in} \quad \Omega_i \setminus \Omega_{12}, \quad \alpha_1 + \alpha_2 = 1 \quad \text{in} \quad \Omega_{12} \tag{8}$$

The dual volume coupling-based continuous Arlequin formulation of the model elasticity problem reads:

$$\text{Find } (\boldsymbol{u}_1,\, \boldsymbol{u}_2,\, \boldsymbol{\Phi}_d) \in \boldsymbol{W}_1 \times \boldsymbol{W}_2 \times \boldsymbol{M}_d\ ;$$

$$\forall\, \boldsymbol{v}_1 \in \boldsymbol{W}_1, \quad a_1(\boldsymbol{u}_1,\, \boldsymbol{v}_1) + c_d(\boldsymbol{\Phi}_d,\, \boldsymbol{v}_1) = \ell_1(\boldsymbol{v}_1) \tag{9}$$

$$\forall\, \boldsymbol{v}_2 \in \boldsymbol{W}_2, \quad a_2(\boldsymbol{u}_2,\, \boldsymbol{v}_2) - c_d(\boldsymbol{\Phi}_d,\, \boldsymbol{v}_2) = \ell_2(\boldsymbol{v}_2) \tag{10}$$

$$\forall\, \boldsymbol{\Psi}_d \in \boldsymbol{M}_d, \quad c_d(\boldsymbol{\Psi}_d,\, \boldsymbol{u}_1 - \boldsymbol{u}_2) = 0 \tag{11}$$

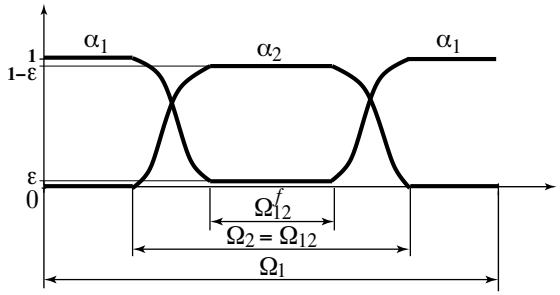

Figure 5: Example of weight parameter functions $\alpha_i,\ (i = 1, 2)$ (see [21, 22] for details on the choice of these functions and the value of $\varepsilon \approx 10^{-2}$, which allows to avoid the ill-conditioning of the operators of the method)

where $\boldsymbol{M}_d$ is the dual *mediator* space of $\boldsymbol{M} = \boldsymbol{W}_1/\Omega_{12}^c = \boldsymbol{W}_2/\Omega_{12}^c = L^2(I; \boldsymbol{V}_{12}^c)$ with $\boldsymbol{V}_{12}^c = \boldsymbol{H}^1(\Omega_{12}^c)$ and $c_d(\cdot\,,\,\cdot)$ is the volume coupling operator:

$$\forall\,(\boldsymbol{\Psi}_d,\,\boldsymbol{v}) \in \boldsymbol{M}_d \times \boldsymbol{M}, \quad c_d(\boldsymbol{\Psi}_d,\,\boldsymbol{v}) = \langle \boldsymbol{\Psi}_d,\,\boldsymbol{v}\rangle_{\boldsymbol{M}_d,\,\boldsymbol{M}} \tag{12}$$

where $\langle\cdot\,,\,\cdot\rangle_{\boldsymbol{M}_d,\,\boldsymbol{M}}$ stands for the duality bracket. The dual volume coupling is a natural mechanical coupling operator, in the sense that, interpreting the Lagrange multiplier field $\boldsymbol{\Phi}_d$ as a density of forces, it has to be in the dual space $\boldsymbol{M}_d$ of the space of the displacements in Ω_{12}^c.

By using the Riesz-Fréchet representation theorem, the natural H^1-scalar product of the space $\boldsymbol{M}$ can be substituted to the duality bracket which leads to:

$$\begin{gathered}
\text{Find } (\boldsymbol{u}_1,\,\boldsymbol{u}_2,\,\boldsymbol{\Phi}) \in \boldsymbol{W}_1 \times \boldsymbol{W}_2 \times \boldsymbol{M}\ ; \\
\forall\,\boldsymbol{v}_1 \in \boldsymbol{W}_1, \quad a_1(\boldsymbol{u}_1,\,\boldsymbol{v}_1) + c(\boldsymbol{\Phi},\,\boldsymbol{v}_1) = \ell_1(\boldsymbol{v}_1) \qquad (13) \\
\forall\,\boldsymbol{v}_2 \in \boldsymbol{W}_2, \quad a_2(\boldsymbol{u}_2,\,\boldsymbol{v}_2) - c(\boldsymbol{\Phi},\,\boldsymbol{v}_2) = \ell_2(\boldsymbol{v}_2) \qquad (14) \\
\forall\,\boldsymbol{\Psi} \in \boldsymbol{M}, \quad c(\boldsymbol{\Psi},\,\boldsymbol{u}_1 - \boldsymbol{u}_2) = 0 \qquad (15)
\end{gathered}$$

where the coupling operator, denoted by $c(\cdot\,,\,\cdot)$, is defined by:

$$\forall(\boldsymbol{\Psi}\,,\boldsymbol{v}) \in \boldsymbol{M} \times \boldsymbol{M}, \quad c(\boldsymbol{\Psi},\boldsymbol{v}) = \int_{\Omega_{12}^c} \kappa(\boldsymbol{\varepsilon}(\boldsymbol{\Psi})\boldsymbol{:}\boldsymbol{\varepsilon}(\boldsymbol{v}) + \frac{1}{e^2}\boldsymbol{\Psi}\cdot\boldsymbol{v})d\Omega \tag{16}$$

where κ is a positive parameter of the order of magnitude of the rigidity of the material (typically the Young modulus E) and e is homogeneous to a length (typically e_{12}^c, the width of the gluing zone, see Figure 4). The choice of the norm and of this width is not at the core of this paper and the guidelines of [21, 22] will be followed. Lagrange multiplier $\boldsymbol{\Phi} \in \boldsymbol{M}$ appearing in (13,14) is homogeneous to a displacement field.

After discretization in space, Problem (13,14,15) can be rewritten using ob-

vious notations:

$$\forall t \in I, \quad \begin{bmatrix} \mathbf{K}_1 & \mathbf{0} & \mathbf{C}_1^T \\ \mathbf{0} & \mathbf{K}_2 & -\mathbf{C}_2^T \\ \mathbf{C}_1 & -\mathbf{C}_2 & \mathbf{0} \end{bmatrix} \begin{bmatrix} \mathbf{u}_1(t) \\ \mathbf{u}_2(t) \\ \mathbf{\Phi}(t) \end{bmatrix} = \begin{bmatrix} \mathbf{F}_1(t) \\ \mathbf{F}_2(t) \\ \mathbf{0} \end{bmatrix} \tag{17}$$

The solution of (17) is denoted $\mathbf{s_{ref}}$. It is usually obtained using a "monolithic" approach which consists in solving directly the previous system that couples the models. Despite the simplicity of implementation, the monolithic approach is not the most appealing approach as it does not allow to use appropriate solvers for each of the super-imposed models. In particular, one can think of the coupling between models such as linear/nonlinear, deterministic/stochastic, atomistic/continuum ...

That is why some works have been proposed in [25] to circumvent this issue by mean of the FETI approach. In the present paper, we propose to use another solver, the LATIN method, to ensure the decoupling of the solution process but also to use reduced-order modeling to solve more efficiently the various models. For that purpose, the Arlequin problem is reformulated as follows.

2.3. Reformulation of the Arlequin problem

Problem (9,10,11) is rewritten by introducing new dual Lagrange multipliers $(\boldsymbol{\Phi}_{d1}, \boldsymbol{\Phi}_{d2}) \in \boldsymbol{M}_d^2$ in the formulation, such that (9,10) reads:

$$\begin{aligned} &\forall \boldsymbol{v}_1 \in \boldsymbol{W}_1, \quad a_1(\boldsymbol{u}_1, \boldsymbol{v}_1) - c_d(\boldsymbol{\Phi}_{d1}, \boldsymbol{v}_1) = \ell_1(\boldsymbol{v}_1) \\ &\forall \boldsymbol{v}_2 \in \boldsymbol{W}_2, \quad a_2(\boldsymbol{u}_2, \boldsymbol{v}_2) - c_d(\boldsymbol{\Phi}_{d2}, \boldsymbol{v}_2) = \ell_2(\boldsymbol{v}_2) \end{aligned} \tag{18}$$

provided that we enforce:

$$\boldsymbol{\Phi}_{d1} + \boldsymbol{\Phi}_{d2} = \mathbf{0} \tag{19}$$

which can be interpreted as the equilibrium in the volume Ω_{12}^c of the densities of forces. Coming back to the primal formulation (13,14,15), new primal Lagrange multipliers $(\boldsymbol{\Phi}_1, \boldsymbol{\Phi}_2) \in \boldsymbol{M}^2$ are introduced such that (13,14) can be rewritten:

$$\begin{aligned} &\forall \boldsymbol{v}_1 \in \boldsymbol{W}_1, \quad a_1(\boldsymbol{u}_1, \boldsymbol{v}_1) - c(\boldsymbol{\Phi}_1, \boldsymbol{v}_1) = \ell_1(\boldsymbol{v}_1) \\ &\forall \boldsymbol{v}_2 \in \boldsymbol{W}_2, \quad a_2(\boldsymbol{u}_2, \boldsymbol{v}_2) - c(\boldsymbol{\Phi}_2, \boldsymbol{v}_2) = \ell_2(\boldsymbol{v}_2) \end{aligned} \tag{20}$$

with:

$$\boldsymbol{\Phi}_1 + \boldsymbol{\Phi}_2 = \mathbf{0} \tag{21}$$

We also introduce new displacement fields $(\boldsymbol{w}_1, \boldsymbol{w}_2) \in \boldsymbol{M}^2$ such that

$$\forall \boldsymbol{\Psi} \in \boldsymbol{M}, \quad c(\boldsymbol{\Psi}, \boldsymbol{w}_i) = c(\boldsymbol{\Psi}, \boldsymbol{u}_i) \tag{22}$$

Equation (22) allows to define the restriction operators $\boldsymbol{\Pi}_i$, $(i = 1, 2)$, that transfer a field defined on space $\boldsymbol{W}_i$ to the mediator space $\boldsymbol{M}$:

$$\boldsymbol{\Pi}_i : \ \boldsymbol{u}_i \in \boldsymbol{W}_i \mapsto \boldsymbol{w}_i = \boldsymbol{\Pi}_i \boldsymbol{u}_i \in \boldsymbol{M} \tag{23}$$

Using these new fields, equation (15) which corresponds to the accommodation between the two models can simply be rewritten as the equality of $\boldsymbol{w}_1$ and $\boldsymbol{w}_2$:

$$\boldsymbol{w}_1 - \boldsymbol{w}_2 = \boldsymbol{0} \tag{24}$$

Then, the Arlequin formulation that will be considered in the next section is:

$$\text{Find} \quad i = (1, 2) \quad (\boldsymbol{u}_i, \boldsymbol{w}_i, \boldsymbol{\Phi}_i) \in \boldsymbol{W}_i \times \boldsymbol{M} \times \boldsymbol{M} \ ;$$

$$\forall \boldsymbol{v}_i \in \boldsymbol{W}_i, \quad a_i(\boldsymbol{u}_i, \boldsymbol{v}_i) - c(\boldsymbol{\Phi}_i, \boldsymbol{v}_i) = \ell_i(\boldsymbol{v}_i), \quad \boldsymbol{w}_i = \boldsymbol{\Pi}_i \boldsymbol{u}_i \tag{25}$$

$$\boldsymbol{w}_1 - \boldsymbol{w}_2 = \boldsymbol{0} \quad \text{and} \quad \boldsymbol{\Phi}_1 + \boldsymbol{\Phi}_2 = \boldsymbol{0} \tag{26}$$

3. Decoupled resolution using the LATIN method

3.1. The LATIN method as a decoupled solver

Problem (25,26) is solved using the LATIN framework. Only the basics of the method are presented in the following and the interested reader can refer to [26] for coupling material subdomains or [19] for coupling multiphysics models. Equation (26) plays the role of an "interface" between the models, which is similar to the interfaces between subdomains and between physics used in these works.

To find the solution $\mathbf{s_{ref}} = \{(\boldsymbol{u}_i, \boldsymbol{w}_i, \boldsymbol{\Phi}_i)\}_{i=1,2}$ of problem (25,26), the idea is a partitioning of the equations by introducing two subsets of elements of $\boldsymbol{W}_1 \times \boldsymbol{M} \times \boldsymbol{M} \times \boldsymbol{W}_2 \times \boldsymbol{M} \times \boldsymbol{M}$. The first one is denoted $\mathbf{A_d}$ and corresponds to the set of solutions to problem (25). The second, denoted $\boldsymbol{\Gamma}$ corresponds to the set of solutions to problem (26). The solution $\mathbf{s_{ref}} = \mathbf{A_d} \cap \boldsymbol{\Gamma}$ is build using an alternated-direction-scheme which consists in finding alternatively an element of $\boldsymbol{\Gamma}$ and an element of $\mathbf{A_d}$. The advantage of this partitioning is mainly that $\mathbf{A_d}$ involves equations that are independent between the two models and $\boldsymbol{\Gamma}$ involve equations that couple the two models but which are defined locally in the accommodation space. This algorithm is sketched in Figure 6.

At iteration $n + 1$, an element $\mathbf{s}_n \in \mathbf{A_d}$ is assumed to be already computed. The algorithm consists of two stages, called *coupled* and *decoupled*. These stages lead to $\hat{\mathbf{s}}_{n+1} \in \boldsymbol{\Gamma}$ and $\mathbf{s}_{n+1} \in \mathbf{A_d}$ and work as follows (subscript i, corresponding

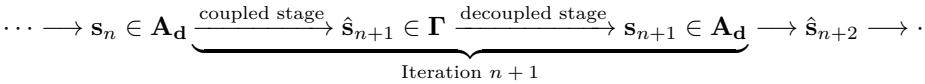

Figure 6: The coupled and decoupled stages of the LATIN method at Iteration $n+1$

to the two models, has to be interpreted as $i = 1, 2$; subscript $n+1$ is skipped to simplify the notations):

Coupled stage. — Knowing a solution $\mathbf{s} \in \mathbf{A_d}$, the coupled stage consists in finding a solution $\hat{\mathbf{s}} \in \mathbf{\Gamma}$ such that a linear search direction $\mathbf{E}^+$ is fulfilled:

$$\hat{\boldsymbol{\Phi}}_i - \boldsymbol{\Phi}_i = k_i(\hat{\boldsymbol{w}}_i - \boldsymbol{w}_i) \tag{27}$$

where $k_i \in \mathbb{R}_+^\star$ are parameters of the method that will be discussed in the following. Recalling the compatibility conditions on the "interface":

$$\hat{\boldsymbol{w}}_1 - \hat{\boldsymbol{w}}_2 = \mathbf{0} \quad \text{and} \quad \hat{\boldsymbol{\Phi}}_1 + \hat{\boldsymbol{\Phi}}_2 = \mathbf{0} \tag{28}$$

the solution at this stage is defined explicitly by:

$$\begin{aligned} \hat{\boldsymbol{w}}_i &= \frac{1}{k_1 + k_2}(\boldsymbol{\varphi}_1 + \boldsymbol{\varphi}_2) \\ \hat{\boldsymbol{\Phi}}_i &= k_i \hat{\boldsymbol{w}}_i - \boldsymbol{\varphi}_i \end{aligned} \tag{29}$$

where $\boldsymbol{\varphi}_i = k_i \boldsymbol{w}_i - \boldsymbol{\Phi}_i$ are known quantities.

Decoupled stage. — Knowing a solution $\hat{\mathbf{s}} \in \mathbf{\Gamma}$, the decoupled stage consists in finding a solution $\mathbf{s} \in \mathbf{A_d}$ such that a linear search direction $\mathbf{E}^-$ is fulfilled:

$$\boldsymbol{\Phi}_i - \hat{\boldsymbol{\Phi}}_i = -k_i(\boldsymbol{w}_i - \hat{\boldsymbol{w}}_i) \tag{30}$$

Recalling the equilibrium equations of the models:

$$\forall \boldsymbol{v}_i \in \boldsymbol{W}_i, \quad a_i(\boldsymbol{u}_i, \boldsymbol{v}_i) - c(\boldsymbol{\Phi}_i, \boldsymbol{v}_i) = \ell_i(\boldsymbol{v}_i), \quad \boldsymbol{w}_i = \boldsymbol{\Pi}_i \boldsymbol{u}_i \tag{31}$$

and using search direction (30) to substitute $\boldsymbol{\Phi}_i$, one obtains:

$$\begin{aligned} \forall \boldsymbol{v}_i \in \boldsymbol{W}_i, \quad a_i(\boldsymbol{u}_i, \boldsymbol{v}_i) - c(\underbrace{\boldsymbol{\Phi}_i}, \boldsymbol{v}_i) &= \ell_i(\boldsymbol{v}_i) \\ -k_i \boldsymbol{w}_i - \hat{\boldsymbol{\alpha}}_i &= -k_i \boldsymbol{\Pi}_i \boldsymbol{u}_i - \hat{\boldsymbol{\alpha}}_i \end{aligned} \tag{32}$$

where $\hat{\boldsymbol{\alpha}}_i = -k_i \hat{\boldsymbol{w}}_i - \hat{\boldsymbol{\Phi}}_i$ are known quantities. One obtains:

$$\forall \boldsymbol{v}_i \in \boldsymbol{W}_i, \quad a_i(\boldsymbol{u}_i, \boldsymbol{v}_i) + c(k_i \boldsymbol{\Pi}_i \boldsymbol{u}_i, \boldsymbol{v}_i) = \ell_i(\boldsymbol{v}_i) - c(\hat{\boldsymbol{\alpha}}_i, \boldsymbol{v}_i) \tag{33}$$

and the decoupled problems to be solved at this stage can be rewritten formally:

$$\text{Find} \quad \boldsymbol{u}_i \in \boldsymbol{W}_i \; ; \quad \forall \boldsymbol{v}_i \in \boldsymbol{W}_i, \quad \boldsymbol{a}_i(\boldsymbol{u}_i, \boldsymbol{v}_i) = \boldsymbol{\ell}_i(\boldsymbol{v}_i) \tag{34}$$

$$\text{Then} \quad (\boldsymbol{w}_i, \boldsymbol{\Phi}_i) \in \boldsymbol{M} \times \boldsymbol{M} \; ; \quad \boldsymbol{w}_i = \boldsymbol{\Pi}_i \boldsymbol{u}_i \quad \text{and} \quad \boldsymbol{\Phi}_i = -k_i \boldsymbol{w}_i - \hat{\boldsymbol{\alpha}}_i \tag{35}$$

where $\boldsymbol{a}_i(\cdot,\cdot) = a_i(\cdot,\cdot) + c(k_i \boldsymbol{\Pi}_i \cdot, \cdot)$ and $\boldsymbol{\ell}_i(\cdot) = \ell_i(\cdot) - c(\hat{\boldsymbol{\alpha}}_i, \cdot)$.

3.2. Some remarks on the algorithm

Initialisation. — The previous algorithm is initialized by assuming that there is no link between the two models. For that purpose, a first decoupled stage is performed to find a solution $\mathbf{s}_0 \in \mathbf{A_d}$ by assuming:

$$\hat{\boldsymbol{w}}_1 = \hat{\boldsymbol{w}}_2 = \mathbf{0} \quad \text{and} \quad \hat{\boldsymbol{\Phi}}_1 = -\hat{\boldsymbol{\Phi}}_2 = \mathbf{0} \tag{36}$$

Convergence indicator. — The convergence of the algorithm is controlled by the indicator η_{LATIN} computed at each iteration:

$$\eta_{\text{LATIN}} = \frac{||\hat{\mathbf{s}} - \mathbf{s}||_{\Omega^c_{12}}}{||\frac{1}{2}(\hat{\mathbf{s}} + \mathbf{s})||_{\Omega^c_{12}}} \tag{37}$$

with the norm $||\mathbf{s}||^2_{\Omega^c_{12}} = ||\boldsymbol{w}_1||^2_{k_1} + ||\boldsymbol{w}_2||^2_{k_2} = \int_{I\times\Omega^c_{12}} \boldsymbol{w}_1 \cdot k_1 \boldsymbol{w}_1 \, dSdt + \int_{I\times\Omega^c_{12}} \boldsymbol{w}_2 \cdot k_2 \boldsymbol{w}_2 \, dSdt$, and the iterations are stopped when the indicator is less than a threshold η (in practice $\eta = 10^{-2}$ in the following numerical examples). Note that, following for example [7], this indicator can also be linked to the error with respect to the reference monolithic solution $\mathbf{s_{ref}}$ but this aspect is out of the scope of this first work on the subject and will be studied in some further works.

Search direction parameters. — In the LATIN method, the choice of the search direction parameters k_i influences the convergence rate of the algorithm and the order of magnitude is chosen following the works on domain decomposition in this framework (see, e.g. [27] or [28] for the case of nonlinearities). During the decoupled stage, the search direction, written in terms of the density of force $\boldsymbol{\Phi}_{di}$ and of the displacement field $\boldsymbol{w}_i$, should be written $\boldsymbol{\Phi}_{di} - \hat{\boldsymbol{\Phi}}_{di} = -k_{di}(\boldsymbol{w}_i - \hat{\boldsymbol{w}}_i)$, where k_{di} is of the order of magnitude of the rigidity of the material (typically the Young modulus) divided by the square of a characteristic length of the coupling area (typically the width of the gluing zone). This leads to k_{di} which is chosen of the order of E/e^{c2}_{12}.

Recalling that the primal field $\boldsymbol{\Phi}$ and the dual field $\boldsymbol{\Phi}_d$ are linked by (16), $\boldsymbol{\Phi}_d$ is of the order of $\kappa/e^2\boldsymbol{\Phi}$. Finally, using the fact that κ is chosen equal to E and e to e^c_{12}, the search direction parameters used in the numerical examples will be $k_1 = k_2 = 1$. The influence of this value will be discussed in the following.

Discretization of the Arlequin formulation. — Classical finite element discretizations are used for spaces $\boldsymbol{W}_i$ with basis functions that are continuous and polynomial by parts over each of the elements. The meshes corresponding to the two models are not *a priori* compatible. A finite element discretization is also introduced for the mediator space $\boldsymbol{M}$. In practice, the latter will often be a restriction of the coarser discretized space, and hence incompatible with the finer discretized mesh, but this is not a requirement. When considering

these incompatible meshes, the integration of the term $c(k_i \mathbf{\Pi}_i \cdot, \cdot)$ in (33) is not classical because it involves functions that may not be polynomials over the elements of any of the meshes. Quadrature methods can therefore not be applied in a straightforward way. Several strategies can be used, for instance by adding adaptively Gauss points to the integration, as done in [29]. In the present work, one prefers to construct the geometrical intersection of the two meshes, as done in [21], so that one falls back on classical integration schemes.

The coupled stage (see Equation (29)) is solved in a strong form, while the decoupled stage (see Equation (34)) is solved in a weak form. The question of the stability of this scheme, in particular when the functional spaces $\boldsymbol{W}_i$ are discretized over incompatible meshes, will be the subject of some theoretical investigations in further works and, herein, we limit ourselves to the apparent stability of the numerical experiments that will be described in Section 4.

3.3. Proper Generalized Decomposition at a glance

During the decoupled stage, the problem to be solved for each model $i = (1, 2)$ is defined by (35), that is the space weak formulation:

$$\text{Find} \quad \boldsymbol{u}_i \in \boldsymbol{W}_i \; ; \quad \forall \boldsymbol{v}_i \in \boldsymbol{W}_i, \quad \boldsymbol{\mathscr{a}}_i(\boldsymbol{u}_i, \boldsymbol{v}_i) = \boldsymbol{\mathscr{\ell}}_i(\boldsymbol{v}_i) \tag{38}$$

where we recall that $\boldsymbol{u}_i$ is a function of $(\boldsymbol{x}, t) \in \Omega_i \times I$, $\boldsymbol{W}_i = L^2(I; \boldsymbol{V}_i)$ and $\boldsymbol{V}_1 = \{\boldsymbol{v}_1 \in \boldsymbol{H}^1(\Omega_1) \; ; \; \boldsymbol{v}_1 = \boldsymbol{0} \text{ on } \Gamma_u\}$ and $\boldsymbol{V}_2 = \boldsymbol{H}^1(\Omega_2)$. We also introduce $\boldsymbol{\mathscr{F}} = L^2(I, \mathbb{R})$ the space of square integrable functions on I.

An approximation of solution $\boldsymbol{u}_i$ is sought using the Proper Generalized Decomposition (PGD) framework. The aim is to find a low-rank approximation of a space-time field as a sum of products of spatial and temporal functions. In our case, space $\boldsymbol{W}_i$ is approximated by $\boldsymbol{\mathcal{S}}_i = \boldsymbol{V}_i \otimes \boldsymbol{\mathscr{F}}$, that is:

$$\boldsymbol{u}_i(\boldsymbol{x}, t) \approx \boldsymbol{u}_i^m(\boldsymbol{x}, t) = \sum_{k=1}^{m} \boldsymbol{\Lambda}_i^k(\boldsymbol{x}) \lambda_i^k(t) \quad \text{where} \quad (\boldsymbol{\Lambda}_i^k, \lambda_i^k) \in \boldsymbol{V}_i \times \boldsymbol{\mathscr{F}} \tag{39}$$

Many choices are possible to build the PGD (Galerkin orthogonality criteria, minimal residual criteria ... [30]). The algorithm which is used herein is based on the Galerkin orthogonality and, for that purpose, a space-time weak formulation of (38) is introduced using the bilinear form A_i and the linear form L_i defined by:

$$A_i(\boldsymbol{u}_i, \boldsymbol{v}_i) = \int_I \boldsymbol{\mathscr{a}}_i(\boldsymbol{u}_i, \boldsymbol{v}_i) dt \quad \text{and} \quad L_i(\boldsymbol{v}_i) = \int_I \boldsymbol{\mathscr{\ell}}_i(\boldsymbol{v}_i) dt \tag{40}$$

The new problem reads:

$$\text{Find} \quad \boldsymbol{u}_i \in \boldsymbol{\mathcal{S}}_i \; ; \quad \forall \boldsymbol{v}_i \in T_{\boldsymbol{u}_i}(\boldsymbol{\mathcal{S}}_{\boldsymbol{i}}), \quad A_i(\boldsymbol{u}_i, \boldsymbol{v}_i) = L_i(\boldsymbol{v}_i) \tag{41}$$

where $T_{\boldsymbol{u}_i}(\boldsymbol{\mathcal{S}_i})$ is the tangent linear space to $\boldsymbol{\mathcal{S}_i}$ at $\boldsymbol{u}_i$. The construction of the solution is done using a greedy procedure. Assuming that a decomposition $\boldsymbol{u}_i^{m-1}$ of order $(m-1)$ is already known:

$$\boldsymbol{u}_i^{m-1} = \sum_{k=1}^{m-1} \boldsymbol{\Lambda}_i^k \lambda_i^k \quad \text{where} \quad (\boldsymbol{\Lambda}_i^k, \lambda_i^k) \in \boldsymbol{V}_i \times \boldsymbol{\mathcal{F}} \tag{42}$$

the solution of (41) is searched in two steps. The first (called *update*) consists in seeking a solution $\bar{\boldsymbol{u}}_i^{m-1}$ of order $(m-1)$ in the reduced-order basis $\{\boldsymbol{\Lambda}_i^k\}_{k=1}^{m-1}$ without any enrichment but only by computating new time functions. The second (called *enrichment*), performed only if the update step is not sufficient, consists in adding a new pair to the decomposition to compute a new solution $\boldsymbol{u}_i^m$ of order m. These steps are described hereafter.

Update step. — Assuming that a decomposition $\boldsymbol{u}_i^{m-1}$ of order $(m-1)$ is known (42), a recombination of the reduced-order basis is searched by computing an approximation $\bar{\boldsymbol{u}}_i^{m-1} = \boldsymbol{u}_i^{m-1} + \sum_{k=1}^{m-1} \boldsymbol{\Lambda}_i^k \bar{\lambda}_i^k$ where only the time functions $\bar{\lambda}_i^k$ have to be searched. For that, a Galerkin orthogonality formulation of (41) is used:

$$\begin{aligned} &\text{Find} \quad \{\bar{\lambda}_i^k\}_{k=1}^{m-1} \in \boldsymbol{\mathcal{F}}^{m-1} \; ; \quad \forall \{\lambda_i^{l\star}\}_{l=1}^{m-1} \in \boldsymbol{\mathcal{F}}^{m-1}, \\ &A_i(\boldsymbol{u}_i^{m-1} + \textstyle\sum_{k=1}^{m-1} \boldsymbol{\Lambda}_i^k \bar{\lambda}_i^k, \sum_{l=1}^{m-1} \boldsymbol{\Lambda}_i^l \lambda_i^{l\star}) = L_i(\sum_{l=1}^{m-1} \boldsymbol{\Lambda}_i^l \lambda_i^{l\star}) \end{aligned} \tag{43}$$

This problem is rewritten:

$$\begin{aligned} &\text{Find} \quad \{\bar{\lambda}_i^k\}_{k=1}^{m-1} \in \boldsymbol{\mathcal{F}}^{m-1} \; ; \quad \forall \{\lambda_i^{l\star}\}_{l=1}^{m-1} \in \boldsymbol{\mathcal{F}}^{m-1}, \\ &A_i(\textstyle\sum_{k=1}^{m-1} \boldsymbol{\Lambda}_i^k \bar{\lambda}_i^k, \sum_{l=1}^{m-1} \boldsymbol{\Lambda}_i^l \lambda_i^{l\star}) = L_i(\sum_{l=1}^{m-1} \boldsymbol{\Lambda}_i^l \lambda_i^{l\star}) - A_i(\boldsymbol{u}_i^{m-1}, \sum_{l=1}^{m-1} \boldsymbol{\Lambda}_i^l \lambda_i^{l\star}) \end{aligned} \tag{44}$$

or, in a more compact form:

$$\begin{aligned} &\text{Find} \quad \{\bar{\lambda}_i^k\}_{k=1}^{m-1} \in \boldsymbol{\mathcal{F}}^{m-1} \; ; \quad \forall \{\lambda_i^{l\star}\}_{l=1}^{m-1} \in \boldsymbol{\mathcal{F}}^{m-1}, \\ &A_i(\textstyle\sum_{k=1}^{m-1} \boldsymbol{\Lambda}_i^k \bar{\lambda}_i^k, \sum_{l=1}^{m-1} \boldsymbol{\Lambda}_i^l \lambda_i^{l\star}) = B_i^m(\sum_{l=1}^{m-1} \boldsymbol{\Lambda}_i^l \lambda_i^{l\star}) \end{aligned} \tag{45}$$

where one introduces $B_i^m(\cdot) = L_i(\cdot) - A_i(\boldsymbol{u}_i^{m-1}, \cdot)$.

It is straightforward to derive that (45) leads to a small system of order $(m-1)$ which can moreover be decoupled provided that $\{\boldsymbol{\Lambda}_i^k\}_{k=1}^{m-1}$ is orthonormalized with respect to the scalar product associated to $\boldsymbol{\mathscr{a}}_i$, that is $\boldsymbol{\mathscr{a}}_i(\boldsymbol{\Lambda}_i^k, \boldsymbol{\Lambda}_i^l) = \delta_{kl}$. The new approximation $\bar{\boldsymbol{u}}_i \approx \bar{\boldsymbol{u}}_i^{m-1}$ being known, the corresponding $\bar{\boldsymbol{w}}_i$ and $\bar{\boldsymbol{\Phi}}_i$ can be computed using the restriction operator and the search direction.

A criterion is then used to check if this recombination of the previous reduced-order basis was sufficient or if an enrichment is required. Reusing the

subscripts introduced in Figure 6 for the consecutive iterations of the LATIN algorithm, this criterion is based on the value of $\xi_i = ||\bar{\boldsymbol{w}}_{i,n+1} - \hat{\boldsymbol{w}}_{i,n+1}||_{k_i} / ||\boldsymbol{w}_{i,n} - \hat{\boldsymbol{w}}_{i,n}||_{k_i}$. If ξ_i is less than a threshold (chosen as 0.9 in the following examples), the enrichment step is skipped and the next iteration of the LATIN algorithm is performed, jumping directly to the next coupled stage. For more details on this aspect, one can refer for example to [31].

Enrichment step. — Assuming now that a new decomposition $\bar{\boldsymbol{u}}_i^{m-1}$ of order $(m-1)$ is known, the reduced-order basis is enriched by seeking an approximation $\boldsymbol{u}_i^m = \bar{\boldsymbol{u}}_i^{m-1} + \Delta\boldsymbol{u} = \bar{\boldsymbol{u}}_i^{m-1} + \boldsymbol{\Lambda}_i \lambda_i$ of order m. For that, a new pair $(\boldsymbol{\Lambda}_i, \lambda_i)$ is added solving:

$$\begin{aligned} &\text{Find} \quad (\boldsymbol{\Lambda}_i, \lambda_i) \in \boldsymbol{V}_i \times \boldsymbol{\mathcal{F}} \; ; \quad \forall (\boldsymbol{\Lambda}_i^\star, \lambda_i^\star) \in \boldsymbol{V}_i \times \boldsymbol{\mathcal{F}}, \\ &A_i(\bar{\boldsymbol{u}}_i^{m-1} + \boldsymbol{\Lambda}_i\lambda_i, \boldsymbol{\Lambda}_i\lambda_i^\star + \boldsymbol{\Lambda}_i^\star\lambda_i) = L_i(\boldsymbol{\Lambda}_i\lambda_i^\star + \boldsymbol{\Lambda}_i^\star\lambda_i) \end{aligned} \tag{46}$$

This problem is rewritten in two equations:

$$\text{Find} \quad (\boldsymbol{\Lambda}_i, \lambda_i) \in \boldsymbol{V}_i \times \boldsymbol{\mathcal{F}} \; ;$$

$$\forall \boldsymbol{\Lambda}_i^\star \in \boldsymbol{V}_i, \quad A_i(\boldsymbol{\Lambda}_i\lambda_i, \boldsymbol{\Lambda}_i^\star\lambda_i) = L_i(\boldsymbol{\Lambda}_i^\star\lambda_i) - A_i(\bar{\boldsymbol{u}}_i^{m-1}, \boldsymbol{\Lambda}_i^\star\lambda_i) \tag{47}$$

$$\forall \lambda_i^\star \in \boldsymbol{\mathcal{F}}, \quad A_i(\boldsymbol{\Lambda}_i\lambda_i, \boldsymbol{\Lambda}_i\lambda_i^\star) = L_i(\boldsymbol{\Lambda}_i\lambda_i^\star) - A_i(\bar{\boldsymbol{u}}_i^{m-1}, \boldsymbol{\Lambda}_i\lambda_i^\star) \tag{48}$$

or, in a more compact form:

$$\text{Find} \quad (\boldsymbol{\Lambda}_i, \lambda_i) \in \boldsymbol{V}_i \times \boldsymbol{\mathcal{F}} \; ;$$

$$\forall \boldsymbol{\Lambda}_i^\star \in \boldsymbol{V}_i, \quad A_i(\boldsymbol{\Lambda}_i\lambda_i, \boldsymbol{\Lambda}_i^\star\lambda_i) = \bar{B}_i^m(\boldsymbol{\Lambda}_i^\star\lambda_i) \tag{49}$$

$$\forall \lambda_i^\star \in \boldsymbol{\mathcal{F}}, \quad A_i(\boldsymbol{\Lambda}_i\lambda_i, \boldsymbol{\Lambda}_i\lambda_i^\star) = \bar{B}_i^m(\boldsymbol{\Lambda}_i\lambda_i^\star) \tag{50}$$

where one introduces $\bar{B}_i^m(\cdot) = L_i(\cdot) - A_i(\bar{\boldsymbol{u}}_i^{m-1}, \cdot)$.

The details of the resolution of nonlinear system (49,50) can be found for example in [27] but, roughly, a fixed-point method initialized by $\lambda_i(t) = 1$ is used. Knowing time function λ_i, Equation (49) allows to compute a space function $\boldsymbol{\Lambda}_i$. Then, knowing space function $\boldsymbol{\Lambda}_i$, Equation (50) allows to compute a time function λ_i. The process can be performed until convergence but, in practice, only 2 iterations are used. Before adding the new pair to the approximation, a Gram-Schmidt algorithm (with respect to the scalar product associated to $\boldsymbol{\omega}_i(\cdot,\cdot)$) is performed. Again, a new approximation $\boldsymbol{u}_i \approx \boldsymbol{u}_i^m$ being known, the corresponding $\boldsymbol{w}_i$ and $\boldsymbol{\Phi}_i$ can be computed using the restriction operator and the search direction.

3.4. Details of the coupled-decoupled strategy

The details of the whole procedure are given in the Algorithm 1.

Algorithm 1: Summary of the procedure, based on a succession of coupled problems to accommodate the models and decoupled problems solved by PGD

begin
  Initialization construction of $\mathbf{s}_0 \in \mathbf{A_d}$
  for $i = 1, 2$ **do**
    Solve decoupled problem (34) for model i to find $(\boldsymbol{u}_i, \boldsymbol{w}_i, \boldsymbol{\Phi}_i)$, assuming $\hat{\boldsymbol{w}}_i = \mathbf{0}$ and $\hat{\boldsymbol{\Phi}}_i = \mathbf{0}$
  $\mathbf{s}_0 = \{(\boldsymbol{u}_i, \boldsymbol{w}_i, \boldsymbol{\Phi}_i)\}_{i=1,2}$
$n \leftarrow 0$
while *error indicator* $\eta_{LATIN} > threshold$ **do**
  begin
    Coupled stage solve coupled problem (29) to find $\{(\hat{\boldsymbol{w}}_i, \hat{\boldsymbol{\Phi}}_i)\}_{i=1,2} \in \boldsymbol{\Gamma}$
  begin
    Decoupled stage solve decoupled problems (38) to find $\mathbf{s}_{n+1} \in \mathbf{A_d}$ using a PGD approach in two steps for each model:
    for $i = 1, 2$ **do**
      Update step: solve (45) for model i, reusing the previous reduced-order basis, to find $(\bar{\boldsymbol{u}}_i, \bar{\boldsymbol{w}}_i, \bar{\boldsymbol{\Phi}}_i)$
      if *skipping criterion* $\xi_i > threshold$ **then**
        Enrichment step: solve system (49,50) for model i to add a new pair and find $(\boldsymbol{u}_i, \boldsymbol{w}_i, \boldsymbol{\Phi}_i) = (\bar{\boldsymbol{u}}_i, \bar{\boldsymbol{w}}_i, \bar{\boldsymbol{\Phi}}_i) + (\Delta\boldsymbol{u}_i, \Delta\boldsymbol{w}_i, \Delta\boldsymbol{\Phi}_i)$
        Orthonormalization of the reduced-order basis of model i
      else
        $(\boldsymbol{u}_i, \boldsymbol{w}_i, \boldsymbol{\Phi}_i) = (\bar{\boldsymbol{u}}_i, \bar{\boldsymbol{w}}_i, \bar{\boldsymbol{\Phi}}_i)$
  $\mathbf{s}_{n+1} = \{(\boldsymbol{u}_i, \boldsymbol{w}_i, \boldsymbol{\Phi}_i)\}_{i=1,2}$
  $n \leftarrow n + 1$

4. Numerical examples

In this section, to illustrate the capabilities of the strategy, we consider two numerical examples of coupling a geometrical local detail in a global structure. The first one is an open-holed plate where two shapes of the hole are considered: round or square. The second is a gamma-shaped structure where the inside corner can have four different designs.

Both examples concern proportional loadings that are, in spite of their simplicity, probably ones of the most common loadings encountered in structural mechanics analysis. In that case, as this first demonstration concerns linear static elasticity, the solution of the monolithic formulation is also proportional and a PGD approach that would apply directly of the coupled monolithic formulation must build a solution with one pair. However, the decoupled treatment of the models leads to a different behavior. During the initialization of the LATIN algorithm, the two models are solved independently, without taking into account of their coupling, which leads to a first PGD mode for each model. The coupling is then recovered iteratively and, for that purpose, new modes are generated. This behavior is similar to that of a classical domain decomposition approach in which the materials subdomains are glued by the mean of interface conditions. The motivation of this choice of proportional loading in the examples is to separate the behavior of the PGD to represent complex solutions from the effect of using a decoupled algorithm to build the different reduced models.

The case of nonlinear problems, such as the coupling between a global linear domain and a local viscoplastic patch, is under investigation. Following our former works on viscoplasticity in the context of the LATIN method, it will only impact the coupled stage of the algorithm, in which the nonlinear evolution law will be also solved. The iterations (and then the modes that will be generated) will allow to satisfy both the nonlinear behavior and the coupling between the models. This aspect will be the subject of a further publication.

4.1. Open-hole plate

In this first example, we come back to the illustration of the introduction, which consists of an open-holed plate simulated under the assumption of plane stress. The two geometries that are considered are presented in Figure 7. The overall dimensions are 100 mm $\times$ 100 mm. The diameter of the round hole and the side length of the square hole are 20 mm. No body force $\boldsymbol{f}$ is considered, but a sinusoidal-cycle linear force $\boldsymbol{F}$ with an amplitude of 10 MPa is prescribed on the right side. The time interval $I = (0, T)$ with $T = 1$ s is discretized using 100 time steps. The material is linear elastic and isotropic with a Young modulus $E = 210$ GPa and a Poisson coefficient $\nu = 0.3$.

Figure 9 illustrates the two possible computational approaches. On the upper part, two different meshes have been generated, to compute the solutions with a monomodel approach. On the lower part, the multimodel simulation is performed using a coarse global model of dimensions 100 mm $\times$ 100 mm and two refined patches of dimensions 50 mm $\times$ 50 mm corresponding to the geometrical details. Apart from the gluing zone which allows to adapt the models to each other, these patches correspond to the zone of interest of the structure (delimited by a red line in the figure) as the stress will be maximum around the hole.

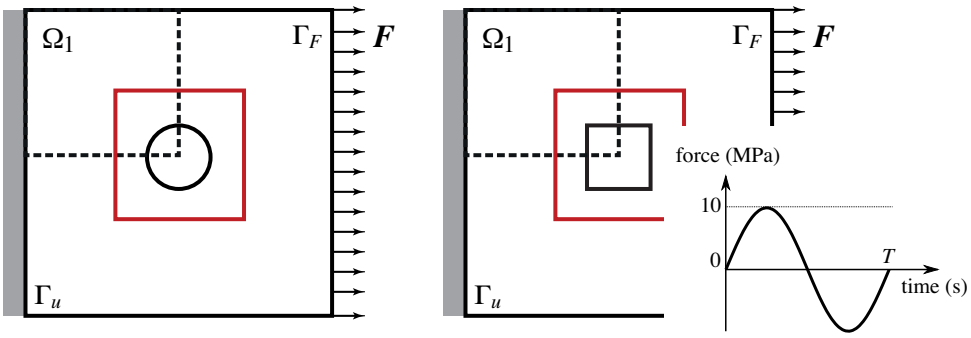

Figure 7: Open-holed plate (the zone of interest is delimited in red)

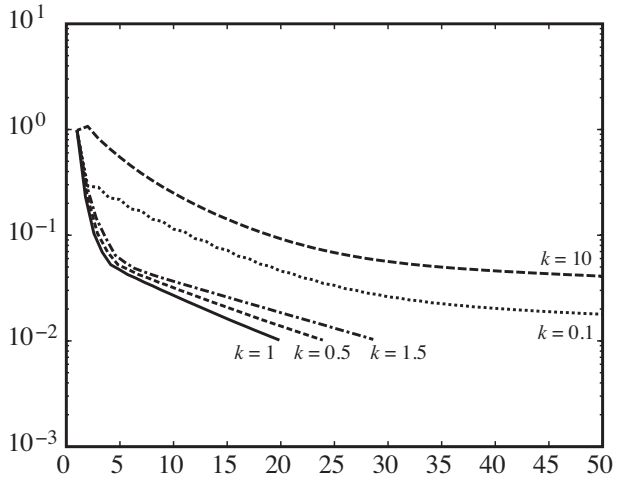

Figure 8: Convergence rate of the algorithm for various values of the search direction parameters $k_1 = k_2 = k$ around the value $k = 1$

The LATIN algorithm is stopped when the indicator $\eta_{LATIN} < \eta = 10^{-2}$. Figure 8 shows the convergence of the algorithm by plotting the evolution of the indicator along the number of iterations. One can notice that the value of the search direction parameters $k_1 = k_2 = k$ influences only slightly the convergence rate around the value $k = 1$ which is selected herein. In future works, in particular including some nonlinearities, further investigations will be derived from the numerous works on this subject in the LATIN method. As already mentioned, the behavior of the algorithm is similar to that of a domain decomposition approach and the advanced techniques (multiscale features, preconditionners ...) that are proposed in the literature to accelerate the convergence of this type of algorithms will be investigated carefully and will certainly lead to an improvement of the convergence rate.

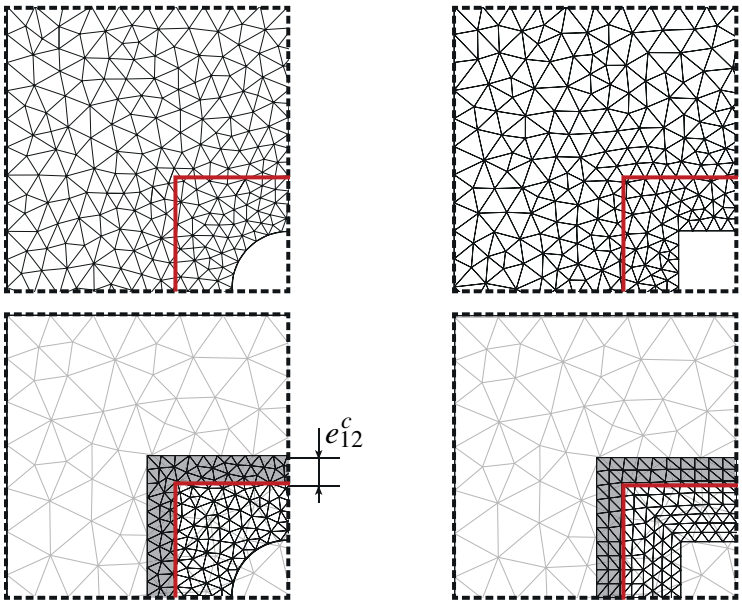

Figure 9: Meshes of 3-nodes triangles with linear interpolation (top: monomodel simulations with 1,696 and 1,644 DOFs; bottom: multimodel approach with a same global mesh with 505 DOFs and two local meshes with 1,016 and 944 DOFs, witdh of the gluing zone $e^c_{12} = 5$ mm) and the zone of interest delimited by a red line

The four first PGD modes generated by the algorithm for each geometry are presented in Figure 10 whereas Figure 11 shows the upper-left quarter of the plate in order to study the zone of interest around the hole at $t = T/4$. One can notice a very good agreement of the Mises stress obtained by the monomodel and the multimodel approach.

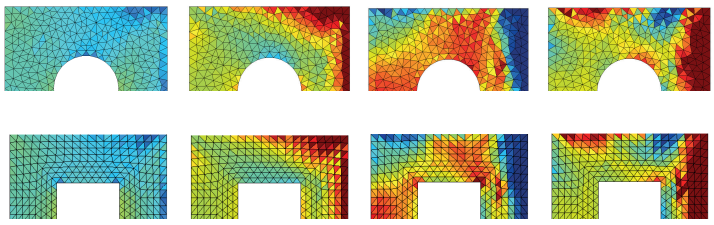

Figure 10: Four first PGD modes for local model 2 $\{\mathbf{\Lambda}^k_2\}_{k=1\ldots4}$, top: for the round hole; bottom: for the square hole, (using the symmetry, only the upper part is represented herein.

4.2. Gamma-shaped structure

The second example consists of a Gamma-shaped structure with four different geometries in the inside corner, presented in Figure 12. The overall

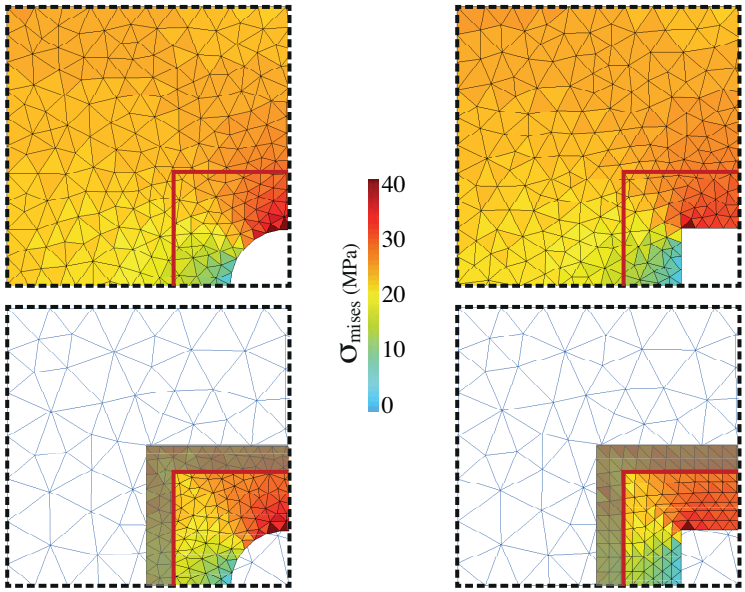

Figure 11: Influence of local geometrical details by embedding local reduced models (Mises stress at $t = T/4$; top: monomodel approach; bottom multimodel simulation)

dimensions are 100 mm $\times$ 100 mm. As in the previous example, no body force $\boldsymbol{f}$ is considered, but a sinusoidal-cycle linear force $\boldsymbol{F}$ with an amplitude of 5 MPa is prescribed on the right side. The time interval $I = (0, T)$ with $T = 1$ s is discretized using 100 time steps. The material is linear elastic and isotropic with a Young modulus $E = 210$ GPa and a Poisson coefficient $\nu = 0.3$.

The same procedure than for the previous case is followed and Figure 13 shows that the various local patches can be embedded in the simulation to study the influence of different shapes and, for example, chose a design which satisfies some prescribed conditions such as the limit of elasticity.

5. Conclusion

In this paper, we investigated the coupling of reduced models for the simulation of structures involving localized geometrical details. For that purpose, we used the Arlequin method to setup a convenient framework to deal with multimodel problems and the LATIN strategy to solve the models independently. This approach allows a very flexible solution of the initial problem. Indeed, different codes can be used to solve the various models and different approaches can be mixed. Herein, the idea was to use the Proper Generalized Decomposition to reduce the computational cost of the models and the promising first

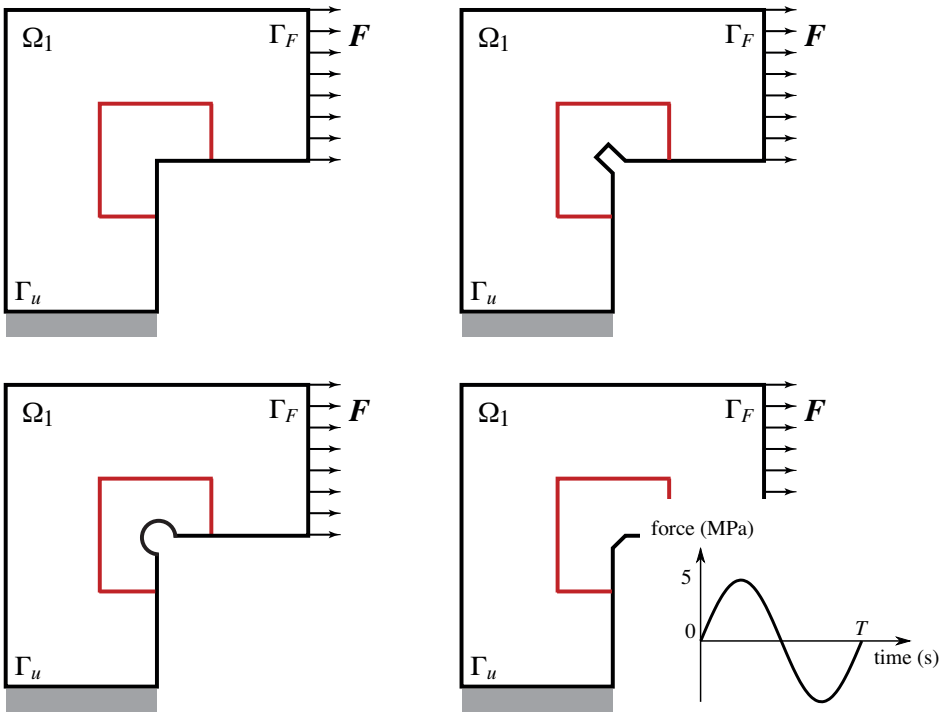

Figure 12: Gamma-shaped structure with different designs in the inside corner (the zone of interest is delimited in red)

numerical results presented in this work show the potential of the approach.

The aim of this first work was to assess the feasibility of the technique and its flexibility, that is why no deep study of the computational gains has been performed, which is the purpose of further works in progress. One of the advantages of the approach is that it permits to use different PGD solvers, dedicated to the specificities of the models that are considered (linear/nonlinear, deterministic/stochastic, atomistic/continuum ...). The coupling of elastic and viscoplastic reduced-order models (following [10]) to capture the nonlinear behavior of material in specific zones is currently under investigation.

In the previous numerical examples, the reduced-order bases corresponding to the two models are built along the iterations of the LATIN algorithm. An interesting approach, that will be investigated in the next future concerns the coupling of different models, some of which being precomputed and stored as PGD modes in a library. This would allow to increase the performances of the strategy and to optimize an industrial structures by exploring the influence of various designs. In that context, some questions will need to be answered such as

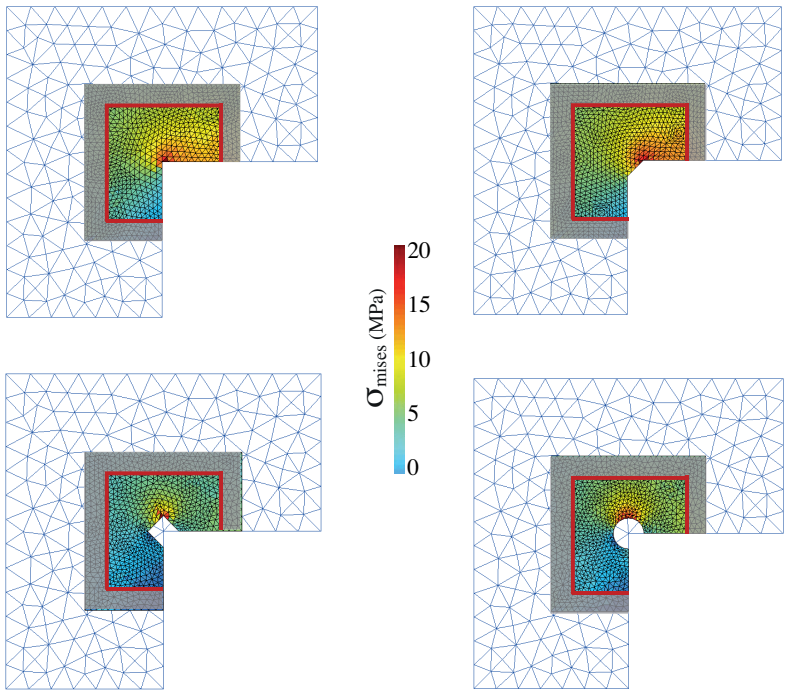

Figure 13: Influence of the local geometrical details by embedding local reduced models (Mises stress at $t = T/4$)

the choice of the coupling zone or of the loadings during the offline construction of the library.

6. Acknowledgments

The authors want to thank the French National Centre for Scientific Research (CNRS) and the French National Research Agency (projet number ANR-14-CE07-0007 CouESt) for the fundings provided to this work.

The numerical simulations were performed using the routines CArl, freely available at `https://github.com/cottereau/CArl`.

References

[1] Y. Maday, E. Ronquist, The reduced-basis element method: application to a thermal fin problem, Journal on Scientific Computing 26(1) (2004)

240–258.

[2] M. Barrault, Y. Maday, N. Nguyen, A. Patera, An "empirical interpolation" method: Application to efficient reduced-basis discretization of partial differential equations, Comptes Rendus Académie des Sciences Paris 339 (2004) 667–672.

[3] T. Lieu, C. Farhat, A. Lesoinne, Reduced-order fluid/structure modeling of a complete aircraft configuration, Computer Methods In Applied Mechanics and Engineering 195 (41-43) (2006) 5730–5742.

[4] M. Gunzburger, J. Peterson, J. Shadid, Reduced-order modeling of time-dependent pdes with multiple parameters in the boundary data, Computational Methods in Applied Mechanics and Engineering 196 (2007) 1030–1047.

[5] A. T. Patera, G. Rozza, Reduced Basis Approximation and A Posteriori Error Estimation for Parametrized Partial Differential Equations. Version 1.0, MIT, 2006.

[6] G. Rozza, K. Veroy, On the stability of the reduced basis method for Stokes equations in parametrized domains, Computational Methods in Applied Mechanics and Engineering 196 (7) (2007) 1244–1260.

[7] P. Ladevèze, Nonlinear Computational Structural Mechanics—New Approaches and Non-Incremental Methods of Calculation, Springer Verlag, 1999.

[8] A. Ammar, B. Mokdad, F. Chinesta, R. Keunings, A new family of solvers for some classes of multidimensional partial differential equations encountered in kinetic theory modeling of complex fluids: Part II: Transient simulation using space-time separated representations, Journal of Non-Newtonian Fluid Mechanics 144 (2-3) (2007) 98–121.

[9] F. Chinesta, P. Ladevèze, E. Cueto, A short review on model order reduction based on proper generalized decomposition, Archives of Computational Methods in Engineering 18 (4) (2011) 395–404.

[10] N. Relun, D. Néron, P.-A. Boucard, A model reduction technique based on the PGD for elastic-viscoplastic computational analysis, Computational Mechanics 51 (1) (2013) 83–92.

[11] M. Cremonesi, D. Néron, P.-A. Guidault, P. Ladevèze, A PGD-based homogenization technique for the resolution of nonlinear multiscale problems, Computer Methods in Applied Mechanics and Engineering 267 (2013) 275–292.

[12] D. Néron, P.-A. Boucard, N. Relun, Time-space PGD for the rapid solution of 3D nonlinear parametrized problems in the many-query context, International Journal for Numerical Methods in Engineering 103 (4) (2015) 275–292.

[13] F. Chinesta, R. Keunings, A. Leygue, The Proper Generalized Decomposition for Advanced Numerical Simulations: a Primer, SpringerBriefs in Applied Sciences and Technology, Springer, 2014.

[14] D. González, I. Alfaro, C. Quesada, E. Cueto, F. Chinesta, Computational vademecums for the real-time simulation of haptic collision between nonlinear solids, Computer Methods in Applied Mechanics and Engineering 283 (1) (2015) 210–223.

[15] I. Alfaro, D. González, F. Bordeu, A. Leygue, A. Ammar, E. Cueto, F. Chinesta, Real-time in silico experiments on gene regulatory networks and surgery simulation on handheld devices, Journal of Computational Surgery 1 (1).

[16] J. V. Aguado, A. Huerta, F. Chinesta, E. Cueto, Real-time monitoring of thermal processes by reduced-order modeling, International Journal For Numerical Methods In Engineering 102 (5) (2015) 991–1017.

[17] A. Ammar, A. Zghal, F. Morel, F. Chinesta, On the space-time separated representation of integral linear viscoelastic models, Comptes Rendus Mécanique 343 (4) (2015) 247–263.

[18] D. Néron, D. Dureisseix, A computational strategy for poroelastic problems with a time interface between coupled physics, International Journal for Numerical Methods in Engineering 73 (6) (2008) 783–804.

[19] D. Néron, D. Dureisseix, A computational strategy for thermo-poroelastic structures with a time-space interface coupling, International Journal for Numerical Methods in Engineering 75 (9) (2008) 1053–1084.

[20] H. Ben Dhia, Multiscale mechanical problems: the Arlequin method (in French), Comptes Rendus de l'Académie des Sciences 326 (1998) 899–904.

[21] H. Ben Dhia, G. Rateau, The Arlequin method as a flexible engineering design tool, International Journal for Numerical Methods in Engineering 62 (2005) 1442–1462.

[22] H. Ben Dhia, Further insights by theoretical investigations of the multiscale arlequin method, International Journal for Multiscale Computational Engineering 6 (3) (2008) 215–232.

[23] R. Cottereau, D. Clouteau, H. Ben Dhia, C. Zaccardi, A stochastic-deterministic coupling method for continuum mechanics, Computer Methods in Applied Mechanics and Engineering 200 (47-48) (2011) 3280–3288.

[24] S. Nazeer, F. Bordeu, A. Leygue, F. Chinesta, Arlequin based PGD domain decomposition, Computational Mechanics 54 (5) (2014) 1175–1190.

[25] H. Ben Dhia, N. Elkhodja, F.-X. Roux, Multimodeling of multi-alterated structures in the arlequin framework. solution with a domain-decomposition solver, European Journal of Computational Mechanics 17 (2008) 969–980.

[26] P. Ladevèze, J.-C. Passieux, D. Néron, The LATIN multiscale computational method and the Proper Generalized Decomposition, Computer Methods in Applied Mechanics and Engineering 199 (2010) 1287–1296.

[27] D. Néron, P. Ladevèze, Proper Generalized Decomposition for multiscale and multiphysics problems, Archives of Computational Methods in Engineering 17 (4) (2010) 351–372.

[28] O. Allix, P. Gosselet, P. Kerfriden, K. Saavedra, Virtual delamination testing through non-linear multi-scale computational methods: Some recent progress, CMC: Computers, Materials & Continua 32 (2) (2012) 107–132.

[29] H. Ben Dhia, G. Rateau, Application of the arlequin method to some structures with defects, European Journal of Computational Mechanics 11 (2-3-4) (2002) 291–304.

[30] A. Nouy, A priori model reduction through proper generalized decomposition for solving time-dependent partial differential equations, Computer Methods In Applied Mechanics and Engineering 199 (23-24) (2010) 1603–1626.

[31] C. Heyberger, P.-A. Boucard, D. Néron, Multiparametric analysis within the proper generalized decomposition framework, Computational Mechanics 49 (3) (2012) 277–289.